

Layer-selective epitaxial self-assembly of porphyrins on ultrathin insulators

L. Ramoino ^{a,*}, M. von Arx ^a, S. Schintke ^a, A. Baratoff ^a, H.-J. Güntherodt ^a, T.A. Jung ^b

^a NCCR Nanoscale Science, Department of Physics, University of Basel, Klingelbergstrasse 82, CH-4056 Basel, Switzerland

^b Laboratory for Micro- and Nanotechnology, Paul Scherrer Institute, CH-5232 Villigen, Switzerland

Received 15 March 2005; in final form 28 September 2005

Available online 19 October 2005

Abstract

Copper-Octaethyl Porphyrin self-assembly has been studied on NaCl islands, 1–3 monolayers thick, grown on metal substrates. Extended ordered molecular monolayers are observed for the first time on ultrathin insulator films. The assembly occurs in hierarchical fashion, starting on the metal substrate, then followed by assembly on the first and second NaCl layers, clearly demonstrating a decrease in adsorption energy for increasing insulator layer thickness. The underlying mechanisms are discussed on the basis of molecule–substrate interactions. Voltage-dependent STM images reveal differences of the electronic structure for molecules adsorbed on metal and NaCl/metal areas.

© 2005 Elsevier B.V. All rights reserved.

1. Introduction

The formation of self-assembled molecular 2D superstructures has been extensively studied on metal substrates, and provided insight into competing intermolecular and molecule–surface interactions as, e.g., van der Waals [1], covalent [2], dipolar or H-bond [3] interactions. To date much less has been reported on molecules adsorbed on insulator surfaces. The few examples of molecular self-assembly on non-conductive substrates focus on small molecules, e.g., CO₂ [4] or CH₄ [5]. Larger organic molecules either do not show any ordering [6,7] or condense in rather large crystallites [8–11]. In a recent publication, assembly of large polar molecules has been induced by trapping them in small pits artificially produced on a KBr surface [12].

A different approach consists in the use of ultrathin insulators, which are particularly interesting because they are suitable for the local investigation of adsorbate properties by Scanning Tunnelling Microscopy (STM) and Spectroscopy (STS). Initial studies reported preferential adsorption

of a perylene derivative on semiconducting CaF₁ monolayers, compared to adsorption on insulating CaF₂ bilayers, both grown on Si(1 1 1) [6]. Furthermore, ultrathin alumina films grown on NiAl(1 1 0), have recently been shown to significantly suppress fluorescence quenching of individual porphyrins by the metal substrate [13]. Investigations of the local electronic structure of ultrathin insulators as a function of layer thickness have suggested that electronic, magnetic and chemical interactions between an adsorbate and the metal could be tuned in a controlled manner by adjusting the number of insulator monolayers [14,15]. Thus, it is of fundamental interest to study the controlled assembly of molecules on ultrathin insulators of various thickness.

In this Letter, we report the assembly of ordered 2D layers of Copper-Octaethyl Porphyrin (CuOEP) molecules on 1–3 layers thick NaCl films, and discuss our results in terms of molecule–surface interactions. NaCl was chosen because its growth behavior on several metal and semiconductor substrates has been well characterized [16–20]. Furthermore, the insulating behavior of NaCl films has been recently demonstrated in STM experiments showing single electron charging of individual gold atoms supported on

* Corresponding author. Fax: +41 61 267 3784.

E-mail address: luca.ramoino@unibas.ch (L. Ramoino).

ultrathin NaCl/Cu(111) [21]. The choice of a molecule from the porphyrin family was motivated by the availability of porphyrins with a large variety of side groups and central metal ions allowing to specifically tune the molecule–substrate interaction. Moreover, the adsorption and self-assembly properties of several porphyrins have already been studied on metal surfaces [22–24].

2. Experiment

STM experiments were performed in a multi-chamber UHV system equipped for in situ sample preparation and characterization by low energy electron diffraction (LEED), ultraviolet photoelectron spectroscopy (UPS), and X-ray photoelectron spectroscopy (XPS). Single crystal metal surfaces, i.e., Cu(111), Ag(001), Ag(111), were prepared by cycles of Ar⁺ sputtering and annealing. Sodium chloride was sublimated from a boron nitride crucible onto the atomically flat and clean metal substrate. The deposition rate (typically 1 Å/min) was monitored by a quartz microbalance while the temperature of the metal substrates was set between 300 and 400 K in order to favor the growth of large 2D NaCl islands. CuOEP was sublimated from a tungsten crucible onto the NaCl/metal substrates kept at room temperature. In a series of experiments, the NaCl mean coverage was varied between 0.3 and 0.7 ML in order

to compare the behavior of CuOEP molecules on bare metal, first and second monolayer salt islands within the same imaged STM frame.

3. Results and discussion

Numerous NaCl/metal samples with various CuOEP coverages, up to a full monolayer, have been investigated at room temperature by STM, LEED, UPS and XPS. In this Letter, a representative selection of the STM data is presented. Unless otherwise stated, we report features commonly observed for CuOEP/NaCl on all three metal substrates.

In zoom-in sequences of STM images both molecular overlayers and square or rectangular shaped NaCl islands can be recognized and their thickness can be determined as illustrated in Fig. 1. The NaCl islands exhibit non-polar edges with some kinks, their surface orientation is equivalent to the non-polar NaCl(001) surface as deduced from lattice resolved STM images obtained before the deposition of CuOEP (not shown here). The lattice constants of the ultrathin NaCl layers have been determined to be 5.53, 5.49, and 5.32 Å on Ag(111), Cu(111) and Ag(001), respectively, consistent with the lateral shrinking earlier observed on Cu(111) [20] and Al(111) [19]. On top of the first salt layer, second and third NaCl layers are observed as

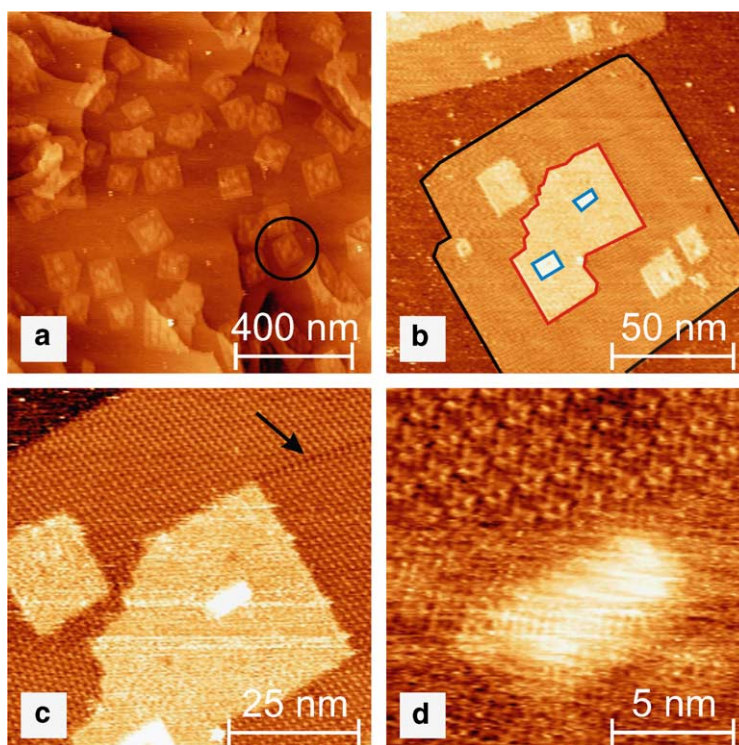


Fig. 1. Zoom-in sequence of STM images referring to the same area for 1 ML CuOEP on NaCl/Ag(111): (a) overview (−0.25 V, 49 pA): NaCl islands of characteristic square shape; (b) zoom-in (−0.34 V, 57 pA) on the island encircled in (a): for clarity, the borders of the NaCl island and of some of its second and third layers are highlighted. The distinctive island shapes allow to univocally identify sample regions of defined NaCl layer thickness, even upon deposition of CuOEP. (c) (−0.34 V, 57 pA) Individually resolved CuOEP molecules self-assembled on the first NaCl layer. The arrow marks an antiphase boundary between two similarly oriented molecular domains. (d) Close up view (−0.25 V, 81 pA) centered on the third NaCl layer: the surrounding second layer is partially covered by ordered molecules.

highlighted in Fig. 1b. The first layer may actually be a double layer as reported for NaCl on Ge(001) [16,18] and on Al(111) [19]. Individually resolved CuOEP molecules form extended domains with a nearly hexagonal superstructure on the NaCl (Fig. 1c,d). Each unit cell accommodates one molecule with its aromatic core parallel to the substrate. Under suitable imaging conditions each molecule exhibits internal structure (Fig. 1d). To our knowledge, our observation represents the first demonstration of extended 2D molecular assembly on ultrathin insulators.

For each metal substrate the close-packed directions of the CuOEP overlayers form specific angles with respect to the NaCl $\langle 100 \rangle$ island edges. Domains related by mirror symmetry with respect to those edges as well as antiphase boundaries are observed (Fig. 1c). This is consistent with point-on-line coincident epitaxy, which appears to be the rule if the lateral stiffness of the molecular overlayer significantly exceeds the shear strength of the overlayer–substrate interface [25]. The simplest superstructure is obtained on NaCl/Ag(001). Based on the measured intermolecular distances and on symmetry analysis, we suggest the model presented in Fig. 2. Adsorption of each molecule centered above a hollow site, as drawn in Fig. 2, (or above bridge sites) provides nearly equivalent adsorption sites for all molecules. This is consistent with the identical appearance of all molecules within the CuOEP layer (Fig. 1c,d). As the observed overlayer periodicity is a half-integer multiple of the substrate periodicity, on-top adsorption would imply alternating adsorption on top of anions and cations, i.e., two quite inequivalent adsorption sites.

In order to gain insight into the self-assembly on different substrate regions we systematically increased the CuOEP mean coverage from 0 to 1 ML. The molecules sequentially adsorb and assemble on the bare metal areas, the first and then the second NaCl layer. This hierarchical behavior is illustrated and summarized in Fig. 3. For a proper interpretation of the STM data it is worth to recall that the tip-sample interaction may strongly affect adsorbates which are not bound stably enough to the substrate. Indeed, when scanning at low CuOEP coverage, we observe a high surface mobility of the molecules, identified by characteristic streak patterns in STM images [26,27]. Only when a threshold coverage on a specific area (i.e., bare metal, first or second NaCl layer) is reached the molecular arrangement is stable enough to be imaged by STM.

Between sample preparation and STM measurements a time ranging from minutes up to two days elapses. The reported observations do not depend on this time interval and also gentle annealing (up to 400 K) did not produce any observable effect. Therefore, we can assume that at the time of our measurements thermodynamic equilibrium between the different sample areas has been reached. The respective adsorption energies per molecule then obey the following inequalities

$$E_{\text{ads}}^{(\text{metal})} > E_{\text{ads}}^{(1^{\text{st}} \text{ layer NaCl})} > E_{\text{ads}}^{(2^{\text{nd}} \text{ layer NaCl})}. \quad (1)$$

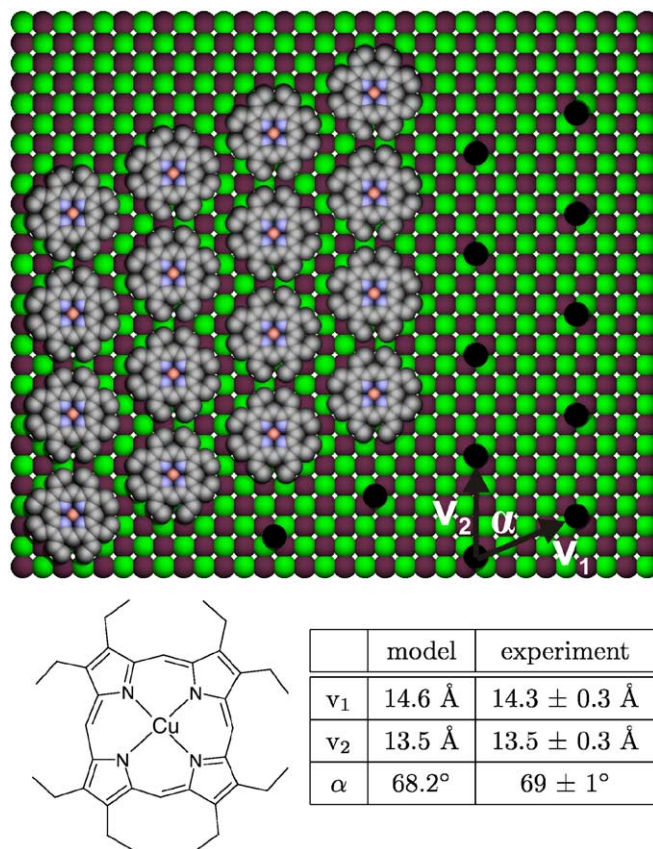


Fig. 2. Schematic model for the superstructure of a CuOEP overlayer on NaCl/Ag(001). The observed registry can be described by the coincidence matrix $M = \begin{pmatrix} 2.5 & 1 \\ 0 & 2.5 \end{pmatrix}$, where the $[100]$ and $[010]$ primitive vectors of the NaCl bulk crystal unit cell have been chosen as basis vectors. The molecule centers are positioned (as also indicated by black dots) for one among several possible sets of twofold symmetric adsorption sites. The in-plane orientation of the molecules could not be determined. The table compares intermolecular distances and angles of the model with those measured by STM.

Moreover, since no 3D molecular aggregates are observed

$$E_{\text{ads}}^{(2^{\text{nd}} \text{ layer NaCl})} > E_{\text{coh}}^{(\text{CuOEP crystal})}, \quad (2)$$

where $E_{\text{coh}}^{(\text{CuOEP crystal})}$ is the cohesive energy per molecule in the CuOEP crystal. The differences between these adsorption energies must be at least in the order of kT (25 meV) as significant population differences are observed at room temperature.

Other mechanisms could in principle lead to the observed hierarchical behavior. In particular step edges, as well as the size of terraces could play a role in the nucleation of stable CuOEP monolayers. The latter can be excluded as several large second NaCl layer islands (lateral dimension > 50 nm) were found, while molecular assembly is observed also on significantly smaller first NaCl layer and clean metal areas. Furthermore, as can be observed in Fig. 1a,b, the step length per unit area for the 1-layer thick NaCl regions (steps between 1- and 2-layer thick terraces) is comparable – if not larger – with the one for bare metal regions (steps between bare metal and 1-layer thick

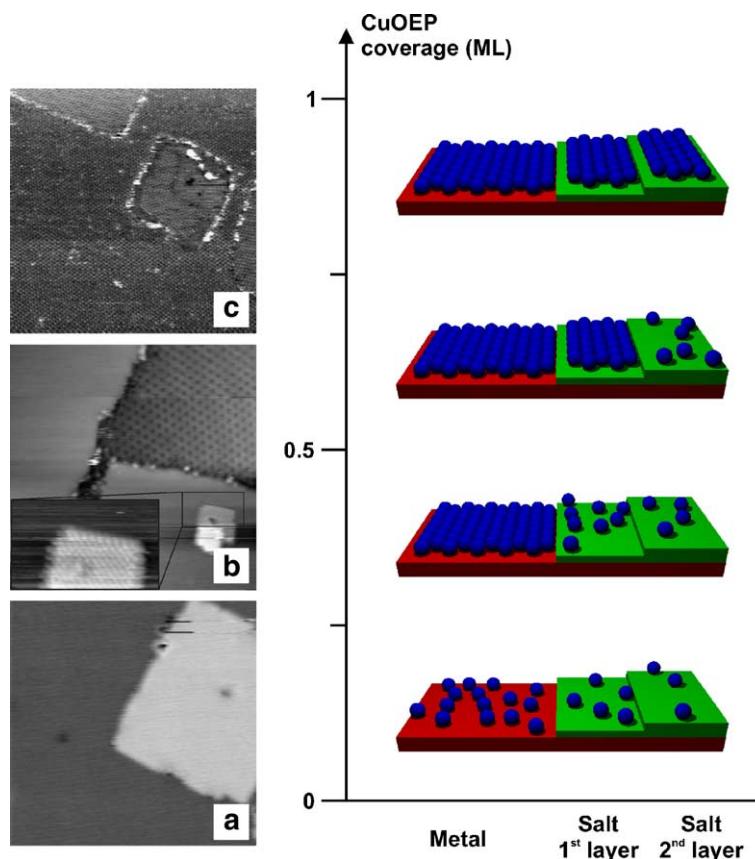


Fig. 3. Schematic illustration of the layer-selective hierarchical assembly of CuOEP as a function of the mean coverage. Epitaxial filling successively occurs on the metal, the first and the second NaCl layer. Stable ordered overlayers are observed on each layer only once it is almost full. This process is explained by the stepwise decrease in adsorption energy of CuOEP. On the left, three STM images acquired for different CuOEP coverage on NaCl/Ag(001) are shown as examples: (a) 0.37 ML (25×25 nm, 1 V, 24 pA): no molecules can be resolved due to their high mobility; (b) 0.67 ML (40×40 nm, -2.9 V, 45 pA): the salt-free metal area is completely covered by assembled molecules but no molecules can be resolved on the NaCl islands. In particular, the second NaCl layer (inset 10×6 nm) appears to be very clean as atomic resolution of NaCl is achieved; (c) 0.84 ML (100×100 nm, -1.6 V, 24 pA): molecular assembly is observed on metal as well as on 1-layer thick NaCl terraces.

NaCl terraces). Therefore, it is very unlikely that nucleation at steps causes the observed sequential adsorption.

Let us discuss the observed selectivity in terms of possible molecule–substrate interactions. For simplicity, we neglect effects of lateral intermolecular interactions on the adsorption energy which are expected to be relatively weak for large flat molecules parallel to the substrate with a small perimeter/area ratio.

For such molecules, van der Waals (vdW) interactions are expected to contribute to the adsorption energy [1]. For chemically inert species adsorbed at a distance d from a flat surface, the vdW attraction is approximately C_3/d^3 . This simple model has successfully been applied to describe the physisorption of rare gases [28]. For a given adsorbate at fixed distance d , it predicts the following difference between the vdW attraction to a metal (m) and to the same metal covered by an insulator (i) of thickness t :

$$(C_{3,m} - C_{3,i}) \left[\frac{1}{d^3} - \frac{1}{(d+t)^3} \right]. \quad (3)$$

For all rare gas atoms, $C_{3,m}$ on Ag(111) is only slightly larger than on Cu(111), but is more than twice $C_{3,i}$ on NaCl

and other alkali halide (001) surfaces [28]. The ratio $C_{3,m}/C_{3,i}$ is essentially independent of the adsorbate and should also be the same for flat molecules. Thus, Eq. (3) appears consistent with the observed decrease of CuOEP adsorption energies.

Porphyrins are however known to have donor character [29]. Therefore, one has to consider an additional electrostatic contribution to $E_{\text{ads}}^{(\text{metal})}$ due to electron transfer from the molecule to the substrate. For CuOEP directly adsorbed on the three metal surfaces studied here, evidence for such a charge transfer comes from the work function decrease observed in UPS measurements [30]. However, there is no evidence for level hybridization, as HOMO and HOMO-1 peaks are rigidly shifted without noticeable changes of their relative intensities and shapes compared to the levels of the free CuOEP molecule.

In principle, a net charge transfer between the molecules and the metal could also take place in presence of an ultra-thin insulator, as electrons can tunnel through a few insulator layers [19,14,31]. However, the broadening of the molecular energy levels is proportional to the tunnelling exponent which governs the decay of the metal local

density of states (LDOS) through the insulator [32,33]. According to Fig. 3b of [19], this decay is about two orders of magnitude per monolayer of NaCl. As a consequence, the HOMO of CuOEP, which lies about 2 eV below the Fermi level [30], is so narrow already for 1 ML NaCl that charge transfer is practically negligible.

To summarize, the differences between adsorption energies on areas covered by 0, 1 or 2 ML of NaCl are most likely explained by charge transfer for molecules directly

adsorbed on the metal and by the vdW energy difference, Eq. (3), once a NaCl layer is present.

In the case of weak substrate–adsorbate interaction, bias-dependent STM experiments have confirmed the expected narrowing of the electronic states for isolated molecules [13,33]. We have acquired STM images on neighboring CuOEP/NaCl/metal and CuOEP/Ag(001) regions (Fig. 4a,d). Such a direct comparison rules out possible artifacts due to tip changes. The round protrusions visible on metal areas stay almost unaffected, while the appearance of molecules adsorbed on NaCl/metal depends on the applied bias (Fig. 4d). This behavior has been repeatedly observed between -0.5 and -2.0 V. Based on symmetry reasons we can argue that this observation is not the result of a modulation by the underlying NaCl pattern (see Fig. 2). Furthermore, in separate experiments on bare NaCl layers (not shown here), no significant changes for similar bias values have been observed. Thus, the molecular appearance and its bias dependence reflect an inherent characteristic of the adsorbed CuOEP, potentially due to decoupling of molecular electronic states from the underlying metal [13,33]. The lack of a clear correlation between the STM contrast and the molecular structure could be due to asymmetry of the tip and/or of the molecular conformation. Detailed calculations and low temperature STM/STS measurements are needed to gain deeper understanding.

4. Conclusions and outlook

The formation of 2D ordered epitaxial molecular layers on ultrathin insulators has been observed for the first time. The reported hierarchical assembly is qualitatively consistent with the rapid decrease in vdW interaction expected for an increased number of insulator layers and with an additional charge transfer to the metal. The observed behavior clearly indicates that the molecule–surface interaction can be discretely tuned by controlled deposition of a few insulator layers between the adsorbate and the metal substrate. Metal–insulator–molecule heterostructures (MIMol) like those investigated here represent interesting model systems to study electronic tunnelling and interactions between molecules and metals across ultrathin insulators on the atomic scale. Such studies are highly relevant for the development of functional molecular electronics.

Acknowledgements

We thank A. Alkauskas for stimulating and helpful discussions, as well as A. Heuri for his engineering and technical support. Nanonis Inc. is acknowledged for the fruitful collaboration on the advanced SPM control system used for these experiments. This work was supported by the National Center of Competence in Research (NCCR) on Nanoscale Sciences and the Swiss National Science Foundation.

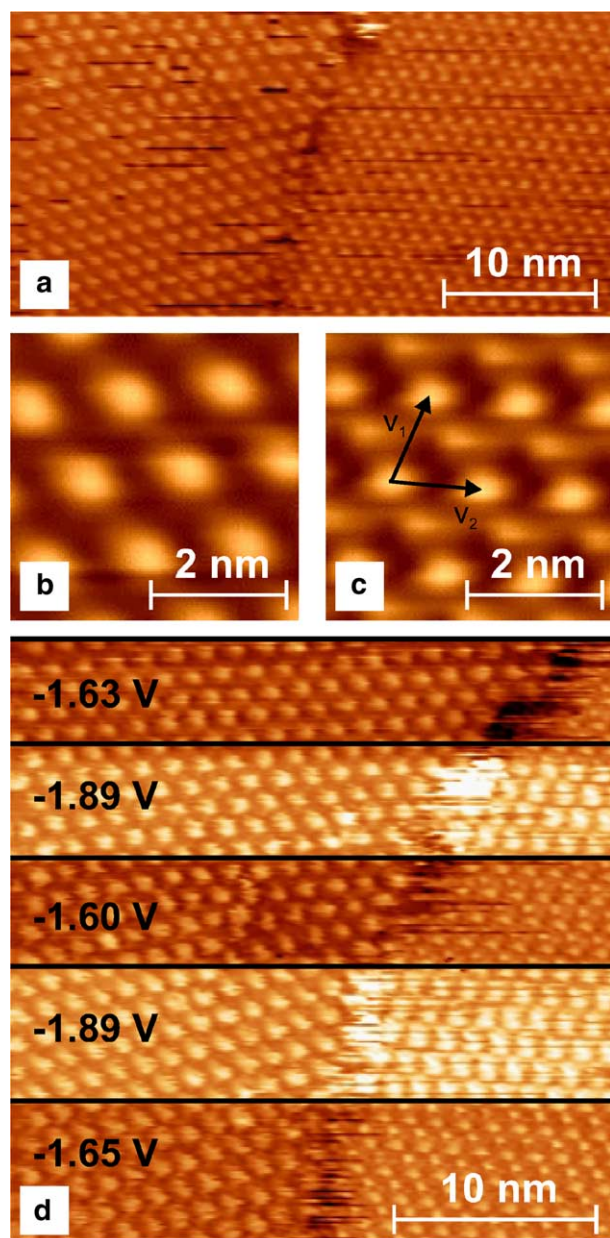


Fig. 4. (a) STM image ($U = -1.76$ V, $I = 40$ pA) across a NaCl–metal step covered by a monolayer of CuOEP. (b) and (c) images are extracted from the left (CuOEP/Ag(001)) and right (CuOEP/NaCl/Ag(001)) parts of image (a) by averaging over several unit cells. The molecular appearance differs depending on the underlying substrate. d) Repeated alternation of the bias voltage between -1.6 and -1.9 V along the slow scan direction (same area as image a) causes changes in appearance only for molecules on NaCl/metal.

References

- [1] S.R. Forrest, Y. Zhang, *Phys. Rev. B* 49 (1994) 11297.
- [2] H. Ozaki, T. Funaki, Y. Mazaki, S. Masuda, Y. Harada, *J. Am. Chem. Soc.* 117 (1995) 5596.
- [3] M. Böhringer, K. Morgenstern, W.-D. Schneider, R. Berndt, F. Mauri, A. De Vita, R. Car, *Phys. Rev. Lett.* 83 (1999) 324.
- [4] J. Schimmelpfennig, S. Fölsch, M. Henzler, *Surf. Sci.* 250 (1991) 198.
- [5] J. Heidberg, O. Schönekas, H. Weiss, G. Lange, J.P. Toennies, *Berich. Bunsen. Gesell.* 99 (1995) 1370.
- [6] H. Rauscher, T.A. Jung, J.-L. Lin, A. Kirakosian, F.J. Himpsel, U. Rohr, K. Müllen, *Chem. Phys. Lett.* 303 (1999) 363.
- [7] C. Tegenkamp, H. Pfnür, *J. Chem. Phys.* 118 (2003) 7578.
- [8] M. Möbus, N. Karl, T. Kobayashi, *J. Cryst. Growth* 116 (1992) 495.
- [9] R. Lüthi, E. Meyer, H. Haefke, L. Howald, W. Gutmannsbauer, H.-J. Güntherodt, *Science* 266 (1994) 1979.
- [10] H. Yanagi, T. Shibutani, *Thin Solid Film* 438–439 (2003) 33.
- [11] F. Balzer, H.-G. Rubahn, *Surf. Sci.* 548 (2004) 170.
- [12] L. Nony, E. Gnecco, A. Baratoff, A. Alkauskas, R. Bennewitz, O. Pfeiffer, S. Maier, A. Wetzol, E. Meyer, Ch. Gerber, *Nanoletters* 4 (2004) 2185.
- [13] X.H. Qiu, G.V. Nazin, W. Ho, *Science* 299 (2003) 542.
- [14] S. Schintke, S. Messerli, M. Pivetta, F. Patthey, L. Libioulle, M. Stengel, A. De Vita, W.-D. Schneider, *Phys. Rev. Lett.* 87 (2001) 276801.
- [15] S. Schintke, W.-D. Schneider, *J. Phys.: Condens. Mat.* 16 (2004) R49, and references therein.
- [16] S. Fölsch, U. Barjenbruch, M. Henzler, *Thin Solid Films* 172 (1989) 123.
- [17] C. Schwenniche, J. Schimmelpfennig, H. Pfnür, *Surf. Sci.* 293 (1993) 57.
- [18] K. Glöckler, M. Sokolowski, A. Soukopp, E. Umbach, *Phys. Rev. B* 54 (1996) 7705.
- [19] H. Hebenstreit, J. Redinger, Z. Horozova, M. Schmidt, R. Poudlouchy, P. Varga, *Surf. Sci.* 424 (1999) L321.
- [20] R. Bennewitz, V. Barwich, M. Bammerlin, C. Loppacher, M. Guggisberg, A. Baratoff, E. Meyer, H.-J. Güntherodt, *Surf. Sci.* 438 (1999) 289.
- [21] J. Repp, G. Meyer, F.E. Olsson, M. Petersson, *Science* 305 (2004) 493.
- [22] T.A. Jung, R.R. Schlittler, J.K. Gimzewski, H. Tang, C. Joachim, *Science* 271 (1996) 181.
- [23] T.A. Jung, R.R. Schlittler, J.K. Gimzewski, *Nature* 386 (1997) 696.
- [24] L. Scudiero, D.E. Barlow, K.W. Hipps, *J. Phys. Chem. B* 106 (2002) 996.
- [25] D.E. Hooks, T. Fritz, M.D. Ward, *Adv. Mater.* 13 (2001) 231.
- [26] M. Böhringer, W.-D. Schneider, R. Berndt, *Surf. Sci.* 408 (1998) 72.
- [27] S. Berner, M. Brunner, L. Ramoino, H. Suzuki, H.-J. Güntherodt, T.A. Jung, *Chem. Phys. Lett.* 348 (2001) 175.
- [28] G. Vidali, G. Ihm, H.-Y. Kim, M.W. Cole, *Surf. Sci. Rep.* 12 (1991) 133.
- [29] H. Ishii, K. Sugiyama, E. Ito, K. Seki, *Adv. Mater.* 11 (1999) 605.
- [30] A. Alkauskas, L. Ramoino, M. von Arx, S. Schintke, A. Baratoff, H.-J. Güntherodt, T.A. Jung, *J. Phys. Chem. B* (submitted).
- [31] F.E. Olsson, M. Persson, *Surf. Sci.* 540 (2003) 172.
- [32] R. Oszwaldowski, J. Ortega, R. Pérez, A. Kahn, H. Vázquez, F. Flores, *Appl. Surf. Sci.* 234 (2004) 107.
- [33] J. Repp, G. Meyer, S.M. Stojković, A. Gourdon, C. Joachim, *Phys. Rev. Lett.* 94 (2005) 026803.